IISE Transactions

ISSN: (Print) (Online) Journal homepage: https://www.tandfonline.com/loi/uiie21

Optimal burn-in policies for multiple dependent degradation processes

Yue Shi, Yisha Xiang, Ying Liao, Zhicheng Zhu & Yili Hong

To cite this article: Yue Shi, Yisha Xiang, Ying Liao, Zhicheng Zhu & Yili Hong (2020): Optimal burn-in policies for multiple dependent degradation processes, IISE Transactions, DOI: 10.1080/24725854.2020.1841344

To link to this article: https://doi.org/10.1080/24725854.2020.1841344

Published online: 09 Dec 2020.

IISE TRANSACTIONS
https://doi.org/10.1080/24725854.2020.1841344

Optimal burn-in policies for multiple dependent degradation processes

Yue Shi[a], Yisha Xiang[a], Ying Liao[a], Zhicheng Zhu[a], and Yili Hong[b]

[a]Texas Tech University, Lubbock, TX, USA; [b]Virginia Tech, Blacksburg, VA, USA

ABSTRACT

Many complex engineering devices experience multiple dependent degradation processes. For each degradation process, there may exist substantial unit-to-unit heterogeneity. In this article, we describe the dependence structure among multiple dependent degradation processes using copulas and model unit-level heterogeneity as random effects. A two-stage estimation method is developed for statistical inference of multiple dependent degradation processes with random effects. To reduce the heterogeneity, we propose two degradation-based burn-in models, one with a single screening point and the other with multiple screening points. At each screening point, a unit is scrapped if one or more degradation levels pass their respective burn-in thresholds. Efficient algorithms are devised to find optimal burn-in decisions. We illustrate the proposed models using experimental data from light-emitting diode lamps. Impacts of parameter uncertainties on optimal burn-in decisions are investigated. Our results show that ignoring multiple dependent degradation processes can cause inferior system performance, such as increased total costs. Moreover, a higher level of dependence among multiple degradation processes often leads to longer burn-in time and higher burn-in thresholds for the two burn-in models. For the multiple-screening-point model, a higher level of dependence can also result in fewer screening points. Our results also show that burn-in with multiple screening points can lead to potential cost savings.

ARTICLE HISTORY
Received 11 September 2019
Accepted 7 October 2020

KEYWORDS
Degradation-based burn-in; multiple screening points; multiple dependent degradation processes; copulas; two-stage estimation method

1. Introduction

The failure of many engineering devices is often the result of gradual and irreversible degradation (Elwany *et al.*, 2011). Complex devices often experience multiple degradation processes, which are naturally dependent due to their structures and shared operational environments, e.g., multiple crack growth on a metal surface of a critical device. Multiple degradation processes are typically competing risks for failure (Wang and Pham, 2012). A device subject to multiple dependent degradation processes is considered to have failed when any degradation level first passes its respective failure threshold. In addition, many complex devices with cutting-edge technologies such as electronic devices have substantial unit-to-unit heterogeneity (Ye *et al.*, 2012). Degradation-based burn-in is an effective approach to reducing the unit-level heterogeneity. However, existing degradation-based burn-in models mainly consider a single degradation process (Tseng and Tang, 2001; Tseng and Peng, 2004; Tsai *et al.*, 2011; Zhang *et al.*, 2015). Burn-in models for multiple dependent degradation processes are rather limited.

In this article, we develop two degradation-based burn-in models for multiple dependent degradation processes with unit-level heterogeneity. We describe the dependence structure among multiple degradation processes using a copula function and model the unit-level heterogeneity as random effects. A two-stage estimation method is developed for statistical inference of multiple dependent degradation processes with random effects. The first burn-in model considers a single screening point and the other considers multiple equi-spaced screening points. Instead of pooling all failure processes together and modeling the overall failure rate, we use different burn-in thresholds for different degradation processes. At each screening point, a device is scrapped if any degradation level exceeds its respective burn-in threshold. A device that survives the burn-in test is released for field use with a warranty period. The objective is to minimize the total expected cost per unit including the expected burn-in cost and the expected operational cost in field use. Note that we use device and unit interchangeably throughout this article. The two main contributions of this article can be summarized as follows:

1. We describe the dependence structure among multiple degradation processes using copulas and model unit-level heterogeneity as random effects. A two-stage estimation method is developed for statistical inference of multiple dependent degradation processes with random effects.
2. We develop two degradation-based burn-in models for multiple dependent degradation processes with unit-level heterogeneity and design efficient algorithms to find optimal burn-in decisions. Our numerical results show that ignoring multiple dependent degradation processes renders the burn-in planning inefficient. In addition, a higher level of dependence among multiple degradation processes often results in a longer burn-in time and higher burn-in thresholds for the two burn-in models. For the multiple-screening-point model, a

CONTACT Yisha Xiang yisha.xiang@ttu.edu

higher level of dependence can also lead to fewer screening points. Our results also show that burn-in with multiple screening points outperforms burn-in with a single screening point in terms of the total expected cost in all test cases considered.

The remainder of this article is organized as follows. Section 2 reviews the relevant literature on multiple dependent degradation processes and degradation-based burn-in models. In Section 3, we model multiple dependent degradation processes with unit-level heterogeneity using the copula method and develop a two-stage estimation approach for statistical inference. In Section 4, we develop two degradation-based burn-in optimization models and design efficient algorithms to find optimal burn-in decisions. A case study of a bivariate degradation model based on experimental degradation data from Light-Emitting Diode (LED) lamps is presented in Section 5. In Section 6, we conduct a sensitivity analysis to examine the necessity of considering multiple dependent degradation processes in burn-in, the impacts of different levels of dependence on optimal burn-in decisions, and the potential cost savings of performing multiple screening points during burn-in. Concluding remarks and future extensions are outlined in Section 7.

2. Literature review

In this section, we review two relevant streams of literature on multiple dependent degradation processes and degradation-based burn-in models.

2.1. Multiple dependent degradation processes

Literature on multiple dependent degradation models (Sari *et al.*, 2009; Zhou *et al.*, 2010; Pan and Balakrishnan, 2011; Wang and Pham, 2012; Pan *et al.*, 2013; Pan and Sun, 2014; Hao *et al.*, 2015; Peng *et al.*, 2016; Fang *et al.*, 2018, 2020) is extensive. Some researchers (Pan and Balakrishnan, 2011; Pan and Sun, 2014) model the joint probability using traditional multivariate distributions. For example, Pan and Balakrishnan (2011) consider two dependent degradation processes, and describe the marginal degradation process by a Gamma process. They approximate the system reliability using a bivariate Birnbaum–Saunders distribution. However, traditional multivariate distributions can only describe linear dependence and require the same form of margins. The copula method has emerged as a flexible and powerful technique to construct complicated dependence structures and allow different forms of margins. Sari *et al.* (2009) develop a bivariate degradation model for LED lighting systems using the Frank copula, and describe the marginal degradation process by a generalized linear model. Zhou *et al.* (2010) describe two degradation processes by using Gamma processes, and model their dependence using the Frank copula. Other papers that examine bivariate degradation models using copulas are Pan *et al.* (2013) and Peng *et al.* (2016), which describe marginal degradation processes by using Wiener processes and inverse Gaussian processes, respectively.

Parameters to be estimated in multivariate degradation models include both univariate degradation parameters and dependence parameters, making statistical inference computationally challenging. Some studies (Zhou *et al.*, 2010; Pan *et al.*, 2011; Pan *et al.*, 2013; Hao *et al.*, 2015) use a Bayesian Markov Chain Monte Carlo (MCMC) method for parameter estimation. Several other studies (Sari *et al.*, 2009; Peng *et al.*, 2016; Fang *et al.*, 2018, 2020) use a two-stage likelihood estimation approach based on the Inference Function for Margins (IFM) method. The IFM method estimates univariate parameters from separate univariate likelihoods, and then estimates dependence parameters from separate bivariate likelihoods or from a multivariate likelihood (Joe and Xu, 1996). For example, Fang *et al.* (2018) develop a two-stage method for the inference of a copula-based multivariate distribution. They estimate univariate parameters for each marginal degradation process using the Maximum Likelihood Estimation (MLE) approch in stage 1 and then infer the copula parameter using the MLE in stage 2.

2.2. Degradation-based burn-in

Degradation-based burn-in has received considerable attention recently. An early degradation-based burn-in model is proposed by Tseng and Tang (2001) using the mixed Wiener process. The model in Tseng and Tang (2001) assumes that a unit is classified as a weak one if its degradation level is below a prespecified burn-in threshold. The optimal burn-in threshold given the burn-in time is determined by minimizing the total misclassification cost including the costs of the type-I and type-II errors of misclassification. Similar degradation-based burn-in policies have also been considered for the mixed integrated Wiener process (Tseng and Peng, 2004), the mixed Gamma process (Tsai *et al.*, 2011), and the mixed inverse Gaussian process (Zhang *et al.*, 2015).

Most degradation-based burn-in models consider a single failure process. Burn-in for multiple failure processes is limited. Ye *et al.* (2012) develop a burn-in planning framework for systems subject to two independent failure processes, a stochastic degradation process and a catastrophic failure process. The catastrophic failure considered in their paper is assumed to cause instant system failure. Hence, only a single degradation process is taken into account for the burn-in planning in their proposed models.

There is a large body of literature on degradation-based burn-in with a single screening point. Only a few studies consider burn-in with multiple screening points. Tseng *et al.* (2003) develop a sequentially inspected burn-in model using a mixed Wiener process, which can eliminate units from a weak subpopulation at early screening times. Cha and Pulcini (2016) propose a new elimination criterion for burn-in with multiple equi-spaced screening points. They consider an elimination level to assess whether an unfailed unit at the end of burn-in belongs to a strong subpopulation given its observed degradation history during the burn-in test.

To the best of our knowledge, multiple dependent degradation processes with unit-to-unit heterogeneity have not been sufficiently considered in the literature, and consequently there is a lack of effective methods for its statistical inference. Degradation-based burn-in models for multiple dependent degradation processes to reduce the heterogeneity also remain limited.

3. Multiple dependent degradation processes with unit-level heterogeneity

Notation

m: number of multiple dependent degradation processes
$\boldsymbol{x}^0$: vector of all initial degradation levels, i.e., $\boldsymbol{x}^0 = (x_1^0, \ldots, x_m^0)$
$\boldsymbol{\xi}$: vector of all failure thresholds, i.e., $\boldsymbol{\xi} = (\xi_1, \ldots, \xi_m)$
$\boldsymbol{X}(t)$: vector of all degradation levels in time [0, t], i.e., $\boldsymbol{X}(t) = (X_1(t), \ldots, X_m(t))$
$F_i(x_i; x_i^0, 0, t)$: marginal Cumulative Distribution Function (CDF) of $X_i(t)$ given $x_i^0, i \in \{1, \ldots, m\}$
$f_i(x_i; x_i^0, 0, t)$: marginal Probability Density Function (PDF) of $X_i(t)$ given $x_i^0, i \in \{1, \ldots, m\}$
$\boldsymbol{\theta}_i$: parameter vector of the ith marginal degradation process, $i \in \{1, \ldots, m\}$
λ: copula parameter(s)
τ: Kendall's tau
t_b: burn-in time for the burn-in model with a single screening point ($\boldsymbol{M}_1$)
γ: burn-in threshold vector for $\boldsymbol{M}_1, \boldsymbol{\gamma} = (\gamma_1, \ldots, \gamma_m)$
q: number of screening points for the burn-in model with multiple screening points $(\boldsymbol{M}_2), q = 2, 3\ldots$
μ: time interval between two consecutive screening points for $\boldsymbol{M}_2$
γ^k: burn-in threshold vector at the kth screening point for $\boldsymbol{M}_2, \boldsymbol{\gamma}^k = (\gamma_1^k, \ldots, \gamma_m^k), k \in \{1, \ldots, q\}$
t_w: warranty period
c_0: inspection cost
c_b: burn-in cost per unit time
c_d: disposal cost
c_f: loss of failure in field use during warranty period
r_w: reward of survival in field use during warranty period
EC_1: total expected cost for $\boldsymbol{M}_1$
EC_2: total expected cost for $\boldsymbol{M}_2$

3.1. Model development

Consider a device that is subject to multiple dependent degradation processes. Each degradation process can be described by a continuous stochastic process. We extend the multiple dependent degradation model in Li and Hao (2016) and Fang *et al.* (2018) by considering unit-to-unit heterogeneity in each marginal degradation process and modeling unit-level heterogeneity as random effects. In this study, it is assumed that a device subject to multiple dependent degradation processes fails when any degradation level first passes its respective failure threshold. Denote the number of the dependent degradation processes by m. Let $\boldsymbol{X}(t)$ represent the vector of all degradation levels in time $[0, t], \boldsymbol{X}(t) = (X_1(t), \ldots, X_m(t))$, where $X_i(t)$ denotes the degradation level of the ith degradation process. Let $\boldsymbol{x}^0$ represent the vector of all initial degradation levels, $\boldsymbol{x}^0 = (x_1^0, \ldots, x_m^0)$, and let $\boldsymbol{\xi}$ represent the vector of all failure thresholds, $\boldsymbol{\xi} = (\xi_1, \ldots, \xi_m)$. We denote the marginal survival probability by $F_i(\xi_i; x_i^0, 0, t), i = 1, \ldots, m$. The joint probability of a device functioning properly at time t, $H(\xi; \boldsymbol{x}^0, 0, t)$, is given by

$$H(\boldsymbol{\xi}; \boldsymbol{x}^0, 0, t) = \Pr\{\boldsymbol{X}(t) \le \boldsymbol{\xi}\} = \Pr\{X_1(t) \le \xi_1, \ldots, X_m(t) \le \xi_m\}.$$

As the degradation processes are dependent, the joint survival probability is not a simple product of all marginal survival probabilities. In this article, we use the copula method to model the dependent relationship among multiple degradation processes. According to Sklar's Theorem in m-dimensions (Nelsen, 2007), the joint survival probability $(H(\cdot))$ can be represented by an m-copula C, which joints all margins $F_i(\xi_i; x_i^0, 0, t), i = 1, \ldots, m$, and is given by

$$H(\boldsymbol{\xi}; \boldsymbol{x}^0, 0, t) = C\Big(F_1(\xi_1; x_1^0, 0, t), \ldots, F_m(\xi_m; x_m^0, 0, t)\Big). \quad (1)$$

Copula functions are generally categorized into two classes: Elliptical copulas and Archimedean copulas (Embrechts *et al.*, 2001). Elliptical copulas, such as the Gaussian copula and Student's t-copula, can capture full pairwise dependence of all marginal distributions and are restricted to have a radial symmetry (Yang *et al.*, 2017). Archimedean copulas, e.g., Frank copula, Clayton copula, and Gumbel copula, only describe the overall dependence among all margins and allow for a great variety of different dependence structures (Yang *et al.*, 2017). For example, the Clayton copula can capture lower tail dependence whereas the Gumbel copula can model upper tail dependence.

3.2. Estimation of unknown parameters

Let $\boldsymbol{\theta}_i$ represent the parameter vector of the ith marginal degradation process, $i = 1, \ldots, m$. For a given copula function C with the copula parameter(s) λ, the parameters to be estimated are represented by the tuple $(\boldsymbol{\theta}_1, \ldots, \boldsymbol{\theta}_m, \lambda)$. Suppose that n units are subject to inspection. Let $X_i(t_{jk})$ represent the degradation level of the ith degradation process of unit j at the kth inspection, $i = 1, \ldots, m, j = 1, \ldots, n$, and $k = 1, \ldots, \zeta_j$. We denote the vector of the ζ_j's degradation increments of the ith degradation process of unit j by $\Delta\boldsymbol{X}_{ij} = (\Delta X_{ij,1}, \ldots, \Delta X_{ij\zeta_j})$, where $\Delta X_{ijk} = X_i(t_{jk}) - X_i(t_{j,k-1})$. The joint CDF and the PDF of $\Delta\boldsymbol{X}_{ij}$ are denoted by $F_{\Delta\boldsymbol{X}_{ij}}(\Delta\boldsymbol{x}_{ij})$ and $f_{\Delta\boldsymbol{X}_{ij}}(\Delta\boldsymbol{x}_{ij})$, respectively. The complete log-likelihood function $l(\boldsymbol{\theta}_1, \ldots, \boldsymbol{\theta}_m, \lambda)$ is given by

$$l(\boldsymbol{\theta}_1, \ldots, \boldsymbol{\theta}_m, \lambda) = \sum_{j=1}^{n} \ln c\big(F_{\Delta\boldsymbol{X}_{1,j}}(\Delta\boldsymbol{x}_{1,j}; \boldsymbol{\theta}_1), \ldots, F_{\Delta\boldsymbol{X}_{mj}}(\Delta\boldsymbol{x}_{mj}; \boldsymbol{\theta}_m); \lambda\big) + \sum_{j=1}^{n}\sum_{i=1}^{m} \ln f_{\Delta\boldsymbol{X}_{ij}}(\Delta\boldsymbol{x}_{ij}; \boldsymbol{\theta}_i), \quad (2)$$

where $c(\cdot)$ is the copula density function.

Due to the complexity of the complete log-likelihood function in Equation (2), it is difficult to estimate all parameters simultaneously by directly using the MLE. To address the computational challenge, MCMC methods have been used in the literature (Zhou *et al.*, 2010; Pan *et al.*, 2011;

Pan *et al.*, 2013; Hao *et al.* 2015) for parameter estimation and work well for many problems. On the other hand, the use of a copula function in the multivariate degradation model makes marginal densities and copula density separable in the log-likelihood function, which suggests that we can first estimate marginal degradation parameters and then infer copula parameters, leading to a two-stage method (Fang *et al.*, 2020). The two-stage method is easy to implement and has been shown to be an effcient estimation approach for multivariate copula-based models (Andersen, 2005; Joe, 2005; Fang *et al.*, 2018; 2020). Therefore, we use a two-stage estimation method for multiple dependent degradation processes with random effects in this study. Specifically, in Stage 1, we first use the semiparametric inference method (Wang, 2010; Wang and Xu, 2010; Ye *et al.*, 2014) to estimate parameters of each marginal degradation process with random effects, which does not require prior knowledge about functional forms of some unknown prameters. The expectation-maximization (EM) algorithm is used to obtain parameter estimates, which has been shown to be an efficient method for random-effects models (Wang, 2010; Wang and Xu, 2010; Ye *et al.*, 2014). Based on the nonparametric estimates of some parameters, we have a better understanding of their functional forms and obtain them by regression. In Stage 2, given a copula function, the copula parameters are then computed using the MLE based on the estimates obtained in Stage 1. The detailed estimation procedure is summarized in Algorithm 1. Note that Equations (3) and (4) are the generic forms in the EM algorithm and their exact forms will be determined when marginal degradation processes are known or determined. We compare the goodness-of-fit of candidate copula functions using Akaike Information Criterion (AIC) (Sakamoto *et al.*, 1986).

Algorithm 1. Determine the unknown parameters $(\hat{\boldsymbol{\theta}}_1, \ldots, \hat{\boldsymbol{\theta}}_m, \hat{\lambda})$

Input: $\boldsymbol{D}_{\text{obs}}, \boldsymbol{D}_{\text{miss}}, \boldsymbol{D}$
Output: $(\hat{\boldsymbol{\theta}}_1, \ldots, \hat{\boldsymbol{\theta}}_m, \hat{\lambda})$
Stage 1. Determine $(\hat{\boldsymbol{\theta}}_1, \ldots, \hat{\boldsymbol{\theta}}_m)$
Initialize ϵ, $(\boldsymbol{\theta}_1^0, \ldots, \boldsymbol{\theta}_m^0), \nu \leftarrow 0$
for $i = 1 : m$ **do**
  repeat
    E-step: compute the Q-function

$$Q(\boldsymbol{\theta}_i|\boldsymbol{\theta}_i^\nu) = E[l(\boldsymbol{\theta}_i; \boldsymbol{D})|\boldsymbol{D}_{\text{obs}}, \boldsymbol{\theta}_i^\nu] \tag{3}$$

    M-step: update $\boldsymbol{\theta}_i^{\nu+1}$

$$\boldsymbol{\theta}_i^{\nu+1} = \arg\max_{\boldsymbol{\theta}_i} Q(\boldsymbol{\theta}_i|\boldsymbol{\theta}_i^\nu) \tag{4}$$

  until $|l(\boldsymbol{\theta}_i^{\nu+1}; \boldsymbol{D}_{\text{obs}}) - l(\boldsymbol{\theta}_i^\nu; \boldsymbol{D}_{\text{obs}})| < \epsilon$
  $\hat{\boldsymbol{\theta}}_i \leftarrow \boldsymbol{\theta}_i^{\nu+1}$
end for
Stage 2. Determine $\hat{\lambda}$
Compute $\hat{\lambda}$ by

$$\hat{\lambda} = \arg\max_{\lambda} \sum_{j=1}^{n} \ln c\left(F_{\Delta X_{1,j}}\left(\Delta \boldsymbol{x}_{1,j}; \hat{\theta}_1\right), \ldots, F_{\Delta X_{mj}}\left(\Delta \boldsymbol{x}_{mj}; \hat{\theta}_{\text{m}}\right); \lambda\right) \tag{5}$$

4. Optimal burn-in policies for multiple dependent degradation processes

In this section, we develop two degradation-based burn-in models for multiple dependent degradation processes, one with a single screening point and the other with multiple screening points. Burn-in with a single screening point eliminates weak units based on degradation information obtained at the end of a burn-in test. Burn-in with multiple screening points can eliminate weak units at early screening points to potentially reduce burn-in costs. We use different burn-in thresholds for different degradation processes. At each screening point, a device is eliminated if any degradation level passes its respective burn-in threshold.

The burn-in cost includes costs of inspection, burn-in and disposal. Let c_0, c_{b}, and c_{d} denote the inspection cost, the burn-in cost per unit time, and the disposal cost, respectively. If a device does not survive the burn-in test, it is scrapped and a disposal cost is incurred. Otherwise, it will be released for field use with a warranty period. Let $t_{\text{w}}, c_{\text{f}}$, and r_{w} represent the warranty period, the loss, and the reward in field use, respectively. If the device fails during the warranty period, the loss is incurred. Otherwise, the reward is gained. We assume that the loss is no less than the disposal cost, i.e., $c_{\text{f}} \geq c_{\text{d}}$. Otherwise, burn-in would not be necessary. It is also assumed that the reward is no less than the negative disposal cost, i.e., $r_{\text{w}} \geq -c_{\text{d}}$. Otherwise, it would be optimal to eliminate all devices in the burn-in test. The objective of the burn-in procedures is to minimize the total expected cost including the expected burn-in cost and the expected operational cost in field use.

4.1. Burn-in with a single screening point

4.1.1. Model development

We first develop the burn-in model with a single screening point. In this model, we consider a burn-in time t_{b} and a burn-in threshold vector $\boldsymbol{\gamma}, \boldsymbol{\gamma} = (\gamma_1, \ldots, \gamma_m)$, where γ_i represents the burn-in threshold of the ith degradation process. The decisions are the burn-in time t_{b} and the burn-in thresholds $\boldsymbol{\gamma}$. The objective is to minimize the total expected cost $EC_1(t_{\text{b}}, \boldsymbol{\gamma})$ including the expected burn-in cost $EC_1^{\text{b}}(t_{\text{b}}, \boldsymbol{\gamma})$ and the expected field operational cost $EC_1^{\text{o}}(t_{\text{b}}, \boldsymbol{\gamma})$. The burn-in optimization model with a single screening point $(\boldsymbol{M}_1)$ is given by

$$\begin{aligned} \min \quad & EC_1(t_{\text{b}}, \boldsymbol{\gamma}) = EC_1^{\text{b}}(t_{\text{b}}, \boldsymbol{\gamma}) + EC_1^{\text{o}}(t_{\text{b}}, \boldsymbol{\gamma}) \\ \text{s.t.} \quad & t_b > 0, \boldsymbol{x}^0 \leq \boldsymbol{\gamma} \leq \boldsymbol{\xi}. \end{aligned} \tag{6}$$

The expected burn-in cost $EC_1^{\text{b}}(t_{\text{b}}, \boldsymbol{\gamma})$ includes the inspection cost, the total burn-in cost, and the expected disposal cost, which is given by

$$\begin{aligned} EC_1^{\text{b}}(t_{\text{b}}, \boldsymbol{\gamma}) &= c_0 + c_{\text{b}} t_{\text{b}} + c_{\text{d}}(1 - \Pr\{\boldsymbol{X}(t_{\text{b}}) \leq \boldsymbol{\gamma}\}) \\ &= c_0 + c_{\text{b}} t_{\text{b}} + c_{\text{d}}\left(1 - H(\boldsymbol{\gamma}; \boldsymbol{x}^0, 0, t_{\text{b}})\right). \end{aligned} \tag{7}$$

The expected field operational cost $EC_1^{\text{o}}(t_{\text{b}}, \boldsymbol{\gamma})$ is the difference between the expected loss and the expected reward in field use. If a device fails during the warranty period, the field operational cost is the loss. If a device survives the warranty period, the field operational cost is the reward. We have $EC_1^o(t_b, \boldsymbol{\gamma})$ as follows

$$\begin{aligned}
&EC_1^o(t_b, \boldsymbol{\gamma}) \\
&= c_f \Pr\{\boldsymbol{X}(t_b) \le \boldsymbol{\gamma}\}(1 - \Pr\{\boldsymbol{X}(t_b + t_w) \le \boldsymbol{\xi} | \boldsymbol{X}(t_b) \le \boldsymbol{\gamma}\}). \\
&\quad - r_w \Pr\{\boldsymbol{X}(t_b) \le \boldsymbol{\gamma}\}\Pr\{\boldsymbol{X}(t_b + t_w) \le \boldsymbol{\xi} | \boldsymbol{X}(t_b) \le \boldsymbol{\gamma}\}) \\
&= c_f H(\boldsymbol{\gamma}; \boldsymbol{x}^0, 0, t_b) - (c_f + r_w) \\
&\quad \times \int_{\boldsymbol{u} \in \mathscr{A}} H(\boldsymbol{\xi}; \boldsymbol{u}, t_b, t_b + t_w) h(\boldsymbol{u}; \boldsymbol{x}^0, 0, t_b) \prod_{i=1}^{m} f_i(u_i; x_i^0, 0, t_b) d\boldsymbol{u},
\end{aligned} \tag{8}$$

where $\boldsymbol{u} = (u_1, ..., u_m)$, $\mathscr{A} = [x_1^0, \gamma_1] \times \cdots \times [x_m^0, \gamma_m]$, and $f_i(\cdot)$ is the PDF derived from the marginal CDF $F_i(\cdot)$.

We first examine the property of the optimal burn-in thresholds given the burn-in time. For a given burn-in time, the optimal burn-in thresholds can be determined using the first-order partial derivatives of the objective function (Equation (6)). Given the other decision variables $(t_b, \gamma_1, ..., \gamma_{i-1}, \gamma_{i+1}, ..., \gamma_m)$, the first-order partial derivative over γ_i is

$$\begin{aligned}
&\frac{\partial}{\partial \gamma_i} EC_1(t_b, \boldsymbol{\gamma}) \\
&= (c_f - c_d) C_i'\Big(F_1(\gamma_1; x_1^0, 0, t_b), ..., F_m(\gamma_m; x_m^0, 0, t_b)\Big) \\
&\quad f_i(\gamma_i; x_i^0, 0, t_b) - (c_f + r_w) \\
&\quad \times f_i(\gamma_i; x_i^0, 0, t_b) \int_{\boldsymbol{u}' \in \mathscr{A}'} H(\boldsymbol{\xi}; \boldsymbol{u}'', t_b, t_b + t_w) h(\boldsymbol{u}''; \boldsymbol{x}^0, 0, t_b) \\
&\quad \prod_{j \ne i} f_j\Big(u_j; x_j^0, 0, t_b\Big) d\boldsymbol{u}',
\end{aligned} \tag{9}$$

where

$$C_i'(\cdot, ..., \cdot) = \frac{\partial C\Big(F_1(\gamma_1; x_1^0, 0, t_b), ..., F_m(\gamma_m; x_m^0, 0, t_b)\Big)}{\partial F_i(\gamma_i; x_i^0, 0, t_b)},$$

$\boldsymbol{u}' = (u_1, ..., u_{i-1}, u_{i+1}, ..., u_m)$, $\mathscr{A}' = [x_1^0, \gamma_1] \times \cdots \times [x_{i-1}^0, \gamma_{i-1}] \times [x_{i+1}^0, \gamma_{i+1}] \times \cdots \times [x_m^0, \gamma_m]$, and $\boldsymbol{u}'' = (u_1, ..., u_{i-1}, \gamma_i, u_{i+1} ..., u_m)$.

As the objective function (Equation (6)) is continuous and differentiable over $\gamma_i \in (x_i^0, \xi_i)$, the optimal burn-in threshold γ_i^* is obtained at either the boundary points (i.e., x_i^0 and ξ_i) or the points in the set $\mathscr{B}_i$ that make Equation (9) equal to zero, where

$$\mathscr{B}_i = \left\{\gamma_i : \rho = \frac{\int_{\boldsymbol{u}' \in \mathscr{A}'} H(\boldsymbol{\xi}; \boldsymbol{u}'', t_b, t_b + t_w) h(\boldsymbol{u}''; \boldsymbol{x}^0, 0, t_b) \prod_{j \ne i} f_j\Big(u_j; x_j^0, 0, t_b\Big) d\boldsymbol{u}'}{C_i'\Big(F_1(\gamma_1; x_1^0, 0, t_b), ..., F_m(\gamma_m; x_m^0, 0, t_b)\Big)}\right\}, \tag{10}$$

and $\rho = (c_f - c_d)/(c_f + r_w)$.

Proposition 1 summarizes how to determine the optimal burn-in threshold γ_i^* given the other decisions $(t_b, \gamma_1, ..., \gamma_{i-1}, \gamma_{i+1}, ..., \gamma_m)$.

Proposition 1. *Consider a device subject to m dependent degradation processes. Given the decisions of the burn-in time and the burn-in thresholds of all degradation processes except the ith degradation process* $(t_b, \gamma_1, ..., \gamma_{i-1}, \gamma_{i+1}, ..., \gamma_m)$, *where* $\gamma_j > x_j^0, \forall j \in \{1, ..., i-1, i+1, ..., m\}$, *the optimal burn-in threshold* γ_i^* *of the ith degradation process in* $\boldsymbol{M}_1$ *is determined by*

$$\gamma_i^* = \underset{\gamma_i \in \{x_i^0, \xi_i\} \cup \mathscr{B}_i}{\arg\min} \; EC_1(t_b, \boldsymbol{\gamma}). \tag{11}$$

Given the burn-in time, we have m decision variables with respect to the burn-in thresholds, which can be iteratively optimized based on Proposition 1 until all decision variables converge or the maximum number of iterations prespecified is reached. In the numerical search procedure, a good starting point is critical to find a high-quality solution. We use the optimal burn-in threshold of each degradation process given the burn-in time as the starting point to search the optimal burn-in thresholds for $\boldsymbol{M}_1$. Next, we show how to obtain the optimal burn-in threshold given the burn-in time for the burn-in model that considers a single degradation process in Proposition 2. Note that a single degradation process is a special case of multiple degradation processes when $m = 1$, and $F(x; x_u, u, t)$ is the CDF of $X(t)$ given the degradation level $X(u) = x_u, t \ge u$. The proof of Proposition 2 is provided in Appendix A.

Proposition 2. *Consider a device subject to a single degradation process. Given the burn-in time* t_b, *the optimal burn-in threshold* γ^* *is determined by* $\rho = F(\xi; \gamma^*, t_b, t_b + t_w)$.

4.1.2. Solution algorithm

We now develop an efficient algorithm to solve the proposed optimization problem with a single screening point ($\boldsymbol{M}_1$). The optimization procedure first performs a line search (e.g., Golden Section Search) to find candidate burn-in times. Given the burn-in time, we use the burn-in threshold provided by Proposition 2 for each degradation process as the starting point, and iteratively optimize the burn-in thresholds one by one based on Proposition 1. The iterative procedure terminates when the convergence criterion regarding all burn-in thresholds is met or the maximum number of iterations is reached. Algorithm 2 summarizes the search procedure to find the optimal burn-in decision $(t_b^*, \boldsymbol{\gamma}^*)$ for $\boldsymbol{M}_1$.

Algorithm 2. Determine the optimal burn-in decision $(t_b^*, \boldsymbol{\gamma}^*)$ for $\boldsymbol{M}_1$

Input: Inspection cost c_0, burn-in cost c_b, disposal cost c_d, failure cost c_f, reward r_w, and warranty period t_w; degradation parameters $(\hat{\boldsymbol{\theta}}_1, ..., \hat{\boldsymbol{\theta}}_m, \hat{\lambda})$, initial degradation levels x^0, and failure thresholds $\boldsymbol{\xi}$;
Output: Optimal burn-in decision $(t_b^*, \boldsymbol{\gamma}^*)$
1: Initialize ϵ and *maxIter*
2: Generate candidate burn-in times $\mathscr{T} = \{t_j; j = 1, ..., J\}$ using a line search
3: **for** $j = 1 : J$ **do**

//Find the optimal burn-in threshold of each degradation process given the burn-in time and use it as the starting point to search the optimal burn-in thresholds for $\boldsymbol{M}_1$

Compute $\tilde{\gamma}_i^*(t_j), i = 1, \ldots, m,$ using Proposition 2;

Initialize $v \leftarrow 0, \gamma_i^0(t_j) \leftarrow \tilde{\gamma}_i^*(t_j), i = 1, \ldots, m;$

while stopping criteria not satisfied **do**

  for $i = 1 : m$ **do**

    Compute $\gamma_i^{v+1}(t_j)$ given $(t_j, \gamma_1^{v+1}(t_j), \ldots, \gamma_{i-1}^{v+1}(t_j), \gamma_{i+1}^{v}(t_j), \ldots, \gamma_m^{v}(t_j))$ using Proposition 1;

  end for

  if $|\gamma_i^{v+1}(t_j) - \gamma_i^{v}(t_j)| < \epsilon, \ \forall i \in \{1, \ldots, m\}$ or $v \geq maxIter$ **then**

    break;

  end if

  $v \leftarrow v + 1$

end while

$\gamma_i^*(t_j) \leftarrow \gamma_i^{v+1}(t_j), i = 1, \ldots, m, \boldsymbol{\gamma}^*(t_j) = (\gamma_1^*(t_j), \ldots, \gamma_m^*(t_j));$

Compute $EC_1(t_j, \boldsymbol{\gamma}^*(t_j))$ based on Equation (6);

end for

Obtain $(t_b^*) = \arg\min_{t_j \in \mathcal{T}} EC_1(t_j, \boldsymbol{\gamma}^*(t_j)), \ \boldsymbol{\gamma}^* = \boldsymbol{\gamma}^*=(t_b^*)$

4.2. Burn-in with multiple screening points

4.2.1. Model development

We next develop the degradation-based burn-in model with multiple screening points. Denote the number of screening points by q, $q \in \{2, 3, \ldots\}$. Devices that survive the qth screening point will be released for field use. We consider equi-spaced screening points with a time interval μ, and the kth screening point thus occurs at time $k\mu$, $k = 1, \ldots, q$. Note that inspection can also be performed sequentially. Let $\boldsymbol{\gamma}^k$ denote the burn-in threshold vector at the kth screening point, $\boldsymbol{\gamma}^k = (\gamma_1^k, \ldots, \gamma_m^k)$. The decisions are the number of screening points q, the time interval μ, and the burn-in thresholds at all screening points $(\boldsymbol{\gamma}^1, \ldots, \boldsymbol{\gamma}^q)$. The objective is to minimize the total expected cost $EC_2(q, \mu, \boldsymbol{\gamma}^1, \ldots, \boldsymbol{\gamma}^q)$ including the expected burn-in cost $EC_2^b(q, \mu, \boldsymbol{\gamma}^1, \ldots, \boldsymbol{\gamma}^q)$ and the expected field operational cost $EC_2^o(q, \mu, \boldsymbol{\gamma}^1, \ldots, \boldsymbol{\gamma}^q)$. The burn-in optimization model with multiple screening points $(\boldsymbol{M}_2)$ is given by

$$\begin{aligned} \min \quad & EC_2(q, \mu, \boldsymbol{\gamma}^1, \ldots, \boldsymbol{\gamma}^q) = EC_2^b(q, \mu, \boldsymbol{\gamma}^1, \ldots, \boldsymbol{\gamma}^q) \\ & + EC_2^o(q, \mu, \boldsymbol{\gamma}^1, \ldots, \boldsymbol{\gamma}^q) \\ \text{s.t.} \quad & q \in \{2, 3, \ldots\}, \mu > 0, \\ & \boldsymbol{x}^0 \leq \boldsymbol{\gamma}^1, \ldots, \boldsymbol{\gamma}^q \leq \boldsymbol{\xi}. \end{aligned} \tag{12}$$

The expected burn-in cost $EC_2^b(q, \mu, \boldsymbol{\gamma}^1, \ldots, \boldsymbol{\gamma}^q)$ is given by

$$EC_2^b(q, \mu, \boldsymbol{\gamma}^1, \ldots, \boldsymbol{\gamma}^q) = \sum_{k=1}^{q} (kc_0 + k\mu c_b + c_d) G(k, \mu, \boldsymbol{\gamma}^1, \ldots, \boldsymbol{\gamma}^k), \tag{13}$$

where $G(k, \mu, \boldsymbol{\gamma}^1, \ldots, \boldsymbol{\gamma}^k)$ represents the probability that a device does not survive the kth screening point. We first derive the probability that a device survives the kth screening point, denoted by $P(k, \mu, \boldsymbol{\gamma}^1, \ldots, \boldsymbol{\gamma}^k)$, as follows:

$$\begin{aligned} & P(k, \mu, \boldsymbol{\gamma}^1, \ldots, \boldsymbol{\gamma}^k) \\ & = \begin{cases} H(\boldsymbol{\gamma}^1; \boldsymbol{x}^0, 0, \mu), & \text{if } k = 1 \\ \int_{\boldsymbol{u}^1 \in \mathcal{A}^1} \cdots \int_{\boldsymbol{u}^{k-1} \in \mathcal{A}^{k-1}} H(\boldsymbol{\gamma}^k; \boldsymbol{u}^{k-1}, (k-1)\mu, k\mu) & \\ \prod_{j=1}^{k-2} h(\boldsymbol{u}^{j+1}; \boldsymbol{u}^j, j\mu, (j+1)\mu) \prod_{i=1}^{m} f_i\left(u_i^{j+1}; u_i^j, j\mu, (j+1)\mu\right) & \\ h(\boldsymbol{u}^1; \boldsymbol{x}^0, 0, \mu) \prod_{i=1}^{m} f_i(u_i^1; x_i^0, 0, \mu) d\boldsymbol{u}^{k-1} \cdots d\boldsymbol{u}^1, & \text{if } 2 \leq k \leq q, \end{cases} \end{aligned} \tag{14}$$

where $\boldsymbol{u}^j = (u_1^j, \ldots, u_m^j)$ for $1 \leq j \leq k-1$, and $\mathcal{A}^1 = [x_1^0, \gamma_1^1] \times \cdots \times [x_m^0, \gamma_m^1]$ and $\mathcal{A}^j = \left[u_1^{j-1}, \gamma_1^j\right] \times \cdots \times \left[u_m^{j-1}, \gamma_m^j\right]$ for $2 \leq j \leq k-1$. Based on Equation (14), we then obtain the probability that a device does not survive the kth screening point $G(k, \mu, \boldsymbol{\gamma}^1, \ldots, \boldsymbol{\gamma}^k)$:

$$\begin{aligned} & G(k, \mu, \boldsymbol{\gamma}^1, \ldots, \boldsymbol{\gamma}^k) \\ & = \begin{cases} 1 - P(1, \mu, \boldsymbol{\gamma}^1), & \text{if } k = 1 \\ P(k-1, \mu, \boldsymbol{\gamma}^1, \ldots, \boldsymbol{\gamma}^{k-1}) - P(k, \mu, \boldsymbol{\gamma}^1, \ldots, \boldsymbol{\gamma}^k), & \text{if } 2 \leq k \leq q. \end{cases} \end{aligned} \tag{15}$$

Similarly, the expected field operational cost $EC_2^o(q, \mu, \boldsymbol{\gamma}^1, \ldots, \boldsymbol{\gamma}^q)$ is given by

$$\begin{aligned} & EC_2^o(q, \mu, \boldsymbol{\gamma}^1, \ldots, \boldsymbol{\gamma}^q) \\ & = c_f\left(P(q, \mu, \boldsymbol{\gamma}^1, \ldots, \boldsymbol{\gamma}^q) - P(q, \mu, t_w, \boldsymbol{\gamma}^1, \ldots, \boldsymbol{\gamma}^q, \boldsymbol{\xi})\right) \\ & \quad - r_w P(q, \mu, t_w, \boldsymbol{\gamma}^1, \ldots, \boldsymbol{\gamma}^q, \boldsymbol{\xi}), \end{aligned} \tag{16}$$

where $P(q, \mu, t_w, \boldsymbol{\gamma}^1, \ldots, \boldsymbol{\gamma}^q, \boldsymbol{\xi})$ represents the probability that a device survives the warranty period and is given by

$$\begin{aligned} & P(q, \mu, t_w, \boldsymbol{\gamma}^1, \ldots, \boldsymbol{\gamma}^q, \boldsymbol{\xi}) \\ & = \int_{\boldsymbol{u}^1 \in \mathcal{A}^1} \cdots \int_{\boldsymbol{u}^q \in \mathcal{A}^q} H(\boldsymbol{\xi}; \boldsymbol{u}^q, q\mu, q\mu + t_w) \prod_{j=1}^{q-1} h(\boldsymbol{u}^{j+1}; \boldsymbol{u}^j, j\mu, (j+1)\mu) \\ & \times \prod_{i=1}^{m} f_i\left(u_i^{j+1}; u_i^j, j\mu, (j+1)\mu\right) h(\boldsymbol{u}^1; \boldsymbol{x}^0, 0, \mu) \\ & \prod_{i=1}^{m} f_i(u_i^1; x_i^0, 0, \mu) d\boldsymbol{u}^q \cdots d\boldsymbol{u}^1. \end{aligned} \tag{17}$$

Computing the total expected cost (Equation (12)) is computationally burdensome because it requires multi-dimensional integration. The maximum number of integrations in Equation (12) is qm. Numerical integration is a common approach to solving multi-dimensional integration problems of an order less than eight (Cools, 2002). When the numbers of degradation processes or screening points become large, simulation approaches (e.g., Monte Carlo simulation) can be used to approximate the total expected cost.

4.2.2. Solution algorithm

An efficient algorithm is designed to solve the multiple-screening-point problem $(\boldsymbol{M}_2)$. We do not expect too many screening points during burn-in and assume that the maximum number of screening points is $q_{\max}$. We use an

Table 1. Light intensity degradation data of 12 LED lamps.

	Inspection time (hr)					
Unit	*0*	*50*	*100*	*150*	*200*	*250*
			Degradation process 1			
1	100	86.6	78.7	76.0	71.6	68.0
2	100	82.1	71.4	65.4	61.7	58.0
3	100	82.7	70.3	64.0	61.3	59.3
4	100	79.8	68.3	62.3	60.0	59.0
5	100	75.1	66.7	62.8	59.0	54.0
6	100	83.7	74.0	67.4	63.0	61.3
			Degradation process 2			
1	100	73.0	65.0	60.7	58.3	58.0
2	100	86.2	67.6	62.7	60.0	59.7
3	100	81.2	65.0	60.6	59.3	57.3
4	100	66.8	63.3	59.3	57.3	56.5
5	100	66.1	64.2	59.4	58.0	55.3
6	100	76.5	61.7	61.3	59.7	56.0

enumeration approach to determine the optimal number of screening points. For each q, a line search is performed to find the time interval (μ) between two consecutive screening points. Given q and μ, we optimize the burn-in thresholds of all degradation processes at all screening points sequentially. We first consider each screening point as the only screening point (as described in $\boldsymbol{M}_1$) and find the optimal burn-in thresholds using Algorithm 2. These burn-in thresholds are used as the starting points to search the optimal burn-in thresholds for $\boldsymbol{M}_2$. At each iteration, we perform a numerical search to improve the burn-in thresholds at each screening point from the first screening point to the last one. At each screening point in any iteration, to accelerate the search process, we use the incumbent burn-in thresholds of each degradation process at the previous screening point (if exists) and the immediate following one (if exists), as the lower and upper bounds, respectively, to search for the burn-in threshold at the current screening point. Such bounds are appropriate because degradation is irreversible. This iterative procedure terminates when the convergence criterion of all burn-in thresholds is met or the maximum number of iterations is reached. Algorithm 3 summarizes the search procedure for $\boldsymbol{M}_2$.

Algorithm 3. Determine the optimal burn-in decision $(q^*, \mu^*, \gamma^{1*}, \ldots, \gamma^{q*})$ for $\boldsymbol{M}_2$

Input: Inspection cost c_0, burn-in cost c_{b}, disposal cost c_{d}, failure cost c_{f}, reward r_{w}, and warranty period t_{w}; degradation parameters $(\hat{\theta}_1, \ldots, \hat{\theta}_m, \hat{\lambda})$, and failure thresholds $\boldsymbol{\xi}$;
Output: Optimal burn-in decision $(q^*, \mu^*, \gamma^{1*}, \ldots, \gamma^{q*})$

Initialize ϵ, *maxIter*, and $q_{\max}$
for $q = 2 : q_{\max}$ **do**
  Generate candidate intervals $\mathscr{T}_q = \left\{\mu_q^j; j = 1, \ldots, J\right\}$ using a line search
  for $j = 1 : J$ **do**
  //Find the optimal burn-in thresholds at each screening point for $\boldsymbol{M}_1$ and use them as the starting points to search the optimal burn-in thresholds for $\boldsymbol{M}_2$
    Compute $\hat{\gamma}^*(k\mu_q^j)$ based on Steps 4-15 in Algorithm 2, $k = 1, \ldots, q$;
    Initialize $v \leftarrow 0$, $\gamma^{k,0} \leftarrow \hat{\gamma}^*(k\mu_q^j)$, $k = 1, \ldots, q$;
    while stopping criteria not satisfied **do**
      for $k = 1 : q$ **do**
        $\gamma^{k,v+1} = \underset{y \in [\gamma^{k-1,v+1}, \gamma^{k+1,v}]}{\operatorname{argmin}} EC_2(q, \mu_q^j, \gamma^{1,v+1}, \ldots, \gamma^{k-1,v+1}, y, \gamma^{k+1,v}, \ldots, \gamma^{q,v})$ via a numerical search, where $\gamma^{0,v+1} = \boldsymbol{x}^0$ and $\gamma^{q+1,v} = \boldsymbol{\xi}$.
      end for
      if $|\gamma_i^{k,v+1} - \gamma_i^{k,v}| < \epsilon$, $\forall i = 1, \ldots, m, k = 1, \ldots, q$ or $v \geq$ *maxIter* **then**
        break;
      end if
      $v \leftarrow v + 1$
    end while
    $\gamma^{k*}\left(k\mu_q^j\right) \leftarrow \gamma^{k,v+1}$, $k = 1, \ldots, q$;
    Compute $EC_2(q, \mu_q^j, \gamma^{1*}(\mu_q^j), \ldots, \gamma^{q*}(q\mu_q^j))$ based on Equation (12);
  end for
end for
Obtain $(q^*, \mu^*) = \underset{q \in \{2, \ldots, q_{\max}\}, \mu_q^j \in \mathscr{T}_q}{\operatorname{argmin}} EC_2(q, \mu_q^j, \gamma^{1*}(\mu_q^j), \ldots, \gamma^{q*}(q\mu_q^j))$, $\gamma^{k^*} = \gamma^{k^*}(k\mu^*)$, $k = 1, \ldots, q^*$

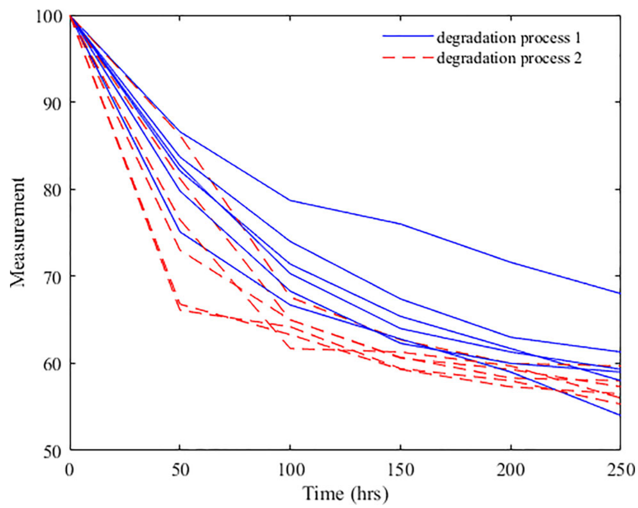

Figure 1. Degradation paths of the LED lamps.

5. Case study

In this section, we provide a case study using LED lamp data to demonstrate a bivariate degradation model and determine optimal burn-in decisions for the two burn-in models. The degradation dataset is from Chaluvadi (2008), where the light intensities of 12 LED lamps are measured every 50 hours up to 250 hours under a current of 40 mA. The degradation data of the 12 LED lamps are shown in Table 1. To demonstrate a bivariate degradation process, several studies in the existing literature (Hao *et al.*, 2015; Fang *et al.*, 2018, 2020) artificially split this dataset by treating it as if the first half represents the first Performance Characteristic (PC) and the other half represents the second PC, and show that there exists a dependence between these two splits. Such a dependence is likely introduced due to the fact that these LED lamps are tested in one chamber with the same operational conditions (e.g., temperature) at the same time. In this article, we use the same approach that artificially splits the dataset in Chaluvadi (2008) into two groups, and consider the first half of it from one degradation process and the other half from another degradation process. Figure 1 shows the degradation paths of the LED lamps with two degradation processes. It is assumed that an LED lamp fails if any degradation level is first below 50 (Chaluvadi, 2008; Hao *et al.*, 2015), i.e., $\boldsymbol{\xi} = (50, 50)$.

5.1. Bivariate degradation model

We assume that each degradation process is governed by a Gamma process with a random effect. For notational convenience, the subscript i for the index of the degradation process is omitted in the following analysis. Consider a Gamma process $\{X(t), t \geq 0\}$ with a time-varying shape parameter $\alpha(t)$ and a rate parameter β, i.e., $Gamma(\alpha(t), \beta)$. The random effect is represented by the rate parameter, which follows a Gamma distribution with a shape parameter κ and a rate parameter δ for mathematical tractability (Lawless and Crowder, 2004), i.e., $\beta \sim Gamma(\kappa, \delta)$. Thus, the unconditional distribution of $\Delta X(t) = X(t+u) - X(t)$ is given by

$$\frac{\kappa(X(t+u) - X(t))}{\delta(\alpha(t+u) - \alpha(t))} \sim F_{2(\alpha(t+u)-\alpha(t)),\, 2\kappa},$$

where $F_{a,b}$ is the F-distribution with degrees of freedom (a, b).

We use the two-stage estimation method proposed in Section 3.2 to estimate the parameters of all marginal degradation processes and the copula parameter. Note that in Stage 1, when using the EM algorithm to estimate parameters of each marginal degradation process, we consider the realizations of the random effect (β) as missing data, i.e., $\boldsymbol{D}_{\text{miss}} = \{\beta_j; j = 1, \ldots, n\}$. The observed dataset is $\boldsymbol{D}_{\text{obs}} = \{x(t_{jk}); j = 1, \ldots, n, k = 1, \ldots, \zeta\}$. In this case, $n = 6$, $\zeta = 5$, and $x(t_{j,0}) = 100, \forall j \in \{1, \ldots, 5\}$. The degradation parameters to be estimated in Stage 1 are $\boldsymbol{\theta} = (\alpha^1 1, \ldots, \alpha^{\zeta}, \alpha^k, \kappa, \delta)$, where $\alpha^k = \alpha(t_k)$, $k = 1, \ldots, \zeta$. Denote $\Delta\alpha^k = \alpha^k - \alpha^{k-1}$, where $\alpha^0 = 0$. The log-likelihood function in Equation (3), up to a constant, given the complete data $\boldsymbol{D}$, is shown as (Ye *et al.*, 2014)

$$l(\boldsymbol{\theta}; \boldsymbol{D}) = l_1(\alpha(\cdot); \boldsymbol{D}) + l_2(\kappa, \delta; \boldsymbol{D}),$$

where

$$l_1(\alpha(\cdot); \boldsymbol{D}) = \sum_{j=1}^{n} \sum_{k=1}^{\zeta} \Big(\Delta\alpha^k (\ln \Delta x_{jk} + \ln \beta_j) - \ln \Gamma(\Delta\alpha^k) \Big), \text{and}$$

$$l_2(\kappa, \delta; \boldsymbol{D}) = \sum_{j=1}^{n} \big(\kappa \ln \delta + (\kappa - 1) \ln \beta_j - \ln \Gamma(\kappa) - \delta\beta_j \big).$$

At the $(v+1)$th iteration of the EM algorithm, we compute $E[\beta_j | \boldsymbol{D}_{\text{obs}}, \boldsymbol{\theta}^v]$ and $E[\ln \beta_j | \boldsymbol{D}_{\text{obs}}, \boldsymbol{\theta}^v]$ in the E-step as follows:

$$E\big[\beta_j | \boldsymbol{D}_{\text{obs}}, \boldsymbol{\theta}^v\big] = \frac{\alpha^{\zeta v} + \kappa^v}{\delta^v + x(t_{j\zeta})}, \text{and}$$

$$E\big[\ln \beta_j | \boldsymbol{D}_{\text{obs}}, \boldsymbol{\theta}^v\big] = \psi(\alpha^{\zeta v} + \kappa^v) - \ln\big(\delta^v + x(t_{j\zeta})\big),$$

where $\psi(\cdot)$ is the digamma function. In the M-step, we update $(\kappa^{v+1}, \delta^{v+1})$ and $\alpha^{v+1}(\cdot)$ by maximizing $E[l_2(\kappa, \delta; \boldsymbol{D}) | \boldsymbol{D}_{\text{obs}}, \boldsymbol{\theta}^v]$ and $E[l_1(\alpha(\cdot); \boldsymbol{D}) | \boldsymbol{D}_{\text{obs}}, \boldsymbol{\theta}^v]$, respectively. Interested readers are referred to Ye *et al.* (2014) for details concerning the semiparametric inference of the Gamma-process model with random effects using the EM algorithm.

Table 2 summarizes the estimates of the two marginal degradation models in Stage 1. Based on the nonparametric estimates of the shape parameter, we assume that the time-varying shape parameter has a form of a power law, i.e., $\alpha_i(t) = a_i t^{b_i}$, $i = 1, 2$. By regression, we obtain the shape parameters of the two degradation processes as $\hat{\alpha}_1(t) = 6.15t^{0.46}$ and $\hat{\alpha}_2(t) = 3.65t^{0.32}$. Based on the estimated marginal degradation models, we then estimate the copula parameter using the MLE in Stage 2. In this article, we use Kendall's tau (τ) to measure the level of dependence between the two degradation processes, which quantifies the association between two random variables. Note that the two degradation processes are independent when $\tau = 0$. For the bivariate degradation model, we consider five commonly used two-dimensional copulas with one parameter: Gaussian copula, Student's t-copula, Frank copula, Clayton copula, and Gumbel copula. Table 3 summarizes the estimates of

Table 2. Estimates of two degradation models.

	Parameters		
	$(\hat{\alpha}^1, \hat{\alpha}^2, \hat{\alpha}^3, \hat{\alpha}^4, \hat{\alpha}^5)$	$\hat{\kappa}$	$\hat{\delta}$
Degradation process 1	(33.52, 52.31, 61.99, 68.82, 73.84)	47.17	25.57
Degradation process 2	(11.93, 16.18, 18.09, 19.42, 20.36)	36.05	74.62

Table 3. Estimates of copula parameters and AIC values.

	$\hat{\lambda}$	τ	AIC	Ranking
Gaussian copula	0.73	0.52	−18.73	3
Student's *t*-copula	0.63	0.43	−15.67	5
Frank copula	20.51	0.82	−21.01	1
Clayton copula	0.64	0.24	−16.36	4
Gumbel copula	2.91	0.66	−18.83	2

the copula parameter $\hat{\lambda}$, and the corresponding values of Kendall's tau and AIC. From Table 3, we can see that the Frank copula has the smallest value of AIC and, therefore, is the most suitable one among the five copulas.

5.2. Optimal burn-in decisions for two degradation processes

Based on the bivariate degradation model, we determine the optimal burn-in decisions for the single-screening-point model ($\boldsymbol{M}_1$) and the multi-screening-point model ($\boldsymbol{M}_2$). We determine the warranty period based on the mean time to failure of an LED lamp, i.e., $t_w = 300$. Note that the LED lamp data used in the case study are obtained under an accelerated degradation test and we use a predetermined warranty period that works for the accelerated degradation processes for demonstration purposes. That is, we treat the accelerated LED lamp data as it were in-field use data during the warranty period, and by setting an in-field use condition to be a current of 40 mA (an accelerated condition) (Chaluvadi, 2008), we obtain a warranty period of 300 hours for the LED lamp data. In practice, the warranty period should be designed for degradation processes under normal operational conditions. The inspection cost is $c_0 = 1$, the burn-in cost per unit time is $c_b = 0.1$, the disposable cost is $c_d = -4$, the loss is $c_f = 100$, and the reward is $r_w = 50$. Table 4 summarizes the optimal burn-in decisions of $\boldsymbol{M}_1$ and $\boldsymbol{M}_2$. From Table 4, we can see that the optimal number of screening points for $\boldsymbol{M}_2$ is two, and the total expected cost of $\boldsymbol{M}_2$ is significantly lower than that of $\boldsymbol{M}_1$. This implies that it may be beneficial to consider multiple screening points during burn-in. We further conduct sensitivity analyses and compare the total expected costs of the two burn-in models under different levels of dependence between the two degradation processes and different values of the inspection cost in the next section.

5.3. Optimal burn-in decisions with consideration of parameter uncertainties

In this case study, the dataset size of the LED lamp example is small, which may lead to large estimation errors. Therefore, we further investigate the impacts of parameter uncertainties on the optimal burn-in decisions. Let $\boldsymbol{\Theta}$ denote the vector of all parameters to be estimated, $\boldsymbol{\Theta} = (\boldsymbol{\theta}_1, ..., \boldsymbol{\theta}_m, \lambda)$. We take into account parameter uncertainties by considering estimated parameters $\hat{\Theta}$ as random variables. The total expected costs from models $\boldsymbol{M}_1$ and $\boldsymbol{M}_2$ are conditional costs given parameter estimates. Denote the conditional costs of $\boldsymbol{M}_1$ and $\boldsymbol{M}_2$ by $EC_1(t_b, \gamma; \hat{\Theta})$ and $EC_2(q, \mu, \gamma^1, ..., \gamma^q; \hat{\Theta})$, respectively. Let $f(\hat{\Theta})$ denote the PDF of the estimated parameters $\hat{\Theta}$. The unconditional costs of $\boldsymbol{M}_1$ and $\boldsymbol{M}_2$ are presented in Equations (18) and (19), respectively.

Table 4. Optimal burn-in decisions for $\boldsymbol{M}_1$ and $\boldsymbol{M}_2$.

Model	q^*	t_b^* or μ^*	γ^* or γ^{1*}	γ^{2*}	EC_1^* or EC_2^*
$\boldsymbol{M}_1$	–	14.12	(10.94,15.94)	–	−9.55
$\boldsymbol{M}_2$	2	12.65	(13.38,15.38)	(14.19,19.38)	−11.68

$$EC_1(t_b, \gamma) = \int EC_1\left(t_b, \gamma; \hat{\Theta}\right) f(\hat{\Theta}) d\hat{\Theta} \tag{18}$$

$$EC_2\left(q, \mu, \gamma^1, ..., \gamma^q\right) = \int EC_2\left(q, \mu, \gamma^1, ..., \gamma^q; \hat{\Theta}\right) f(\hat{\Theta}) d\hat{\Theta} \tag{19}$$

The form of $f(\hat{\Theta})$ is complicated, and therefore it is very difficult to derive closed-form expressions of Equations (18) and (19). We use the method in Ye *et al.* (2012) to approximate the unconditional costs. Specifically, we use the bootstrap to generate 1000 sample estimates by resampling from the original LED lamp data, and each sample has the same sample size as the original dataset. Table 5 summarizes the mean and standard deviation of each parameter. We compute the conditional costs of $\boldsymbol{M}_1$ and $\boldsymbol{M}_2$ for each sample estimate and approximate the unconditional cost of each burn-in model as the average of the 1000 conditional costs. Note that Proposition 1 is no longer applicable for $\boldsymbol{M}_1$ with the unconditional cost to determine the optimal burn-in threshold for each degradation process due to the extreme difficulty in finding optimal decisions using derivative-based methods. Therefore, we modify Algorithm 2 to obtain optimal burn-in decisions. The optimal burn-in thresholds of all degradation processes given the burn-in time are optimized using derivative-free numerical search methods instead of using Proposition 1. The optimal burn-in decisions of the two burn-in models considering parameter uncertainties are shown in Table 6. From Table 6, we observe a similar pattern that the total expected cost of $\boldsymbol{M}_2$ is lower than that of $\boldsymbol{M}_1$, as shown in Table 4. Moreover, comparing the optimal burn-in decisions in Table 4 with those in Table 6, we can see that there is no significant difference of the optimal burn-in decisions with and without considering parameter uncertainties. Our analysis shows that the optimal burn-in decisions in the LED lamp example are not sensitive to the change in the parameters of degradation distributions.

6. Sensitivity analyses

In this section, we first examine whether it is necessary to consider multiple dependent degradation processes in burn-in, and then investigate the impacts of different levels of

Table 5. The mean and standard deviation of parameters.

Parameters	$\hat{a}_1$	$\hat{b}_1$	$\hat{\kappa}_1$	$\hat{\delta}_1$	$\hat{a}_2$	$\hat{b}_2$	$\hat{\kappa}_2$	$\hat{\delta}_2$	$\hat{\lambda}$
Mean	9.96	0.45	52.14	18.43	5.44	0.31	40.35	64.30	23.42
Standard deviation	3.23	0.02	9.18	4.40	3.42	0.05	6.03	13.15	13.84

Table 6. Optimal burn-in decisions for $\boldsymbol{M}_1$ and $\boldsymbol{M}_2$ considering parameter uncertainties.

Model	q^*	t_b^* or μ^*	γ^* or γ^{1*}	γ^{2*}	EC_1^* or EC_2^*
$\boldsymbol{M}_1$	–	14.52	(11.37, 18.62)	–	−11.04
$\boldsymbol{M}_2$	2	11.55	(12.24, 20.28)	(13.97, 21.56)	−11.89

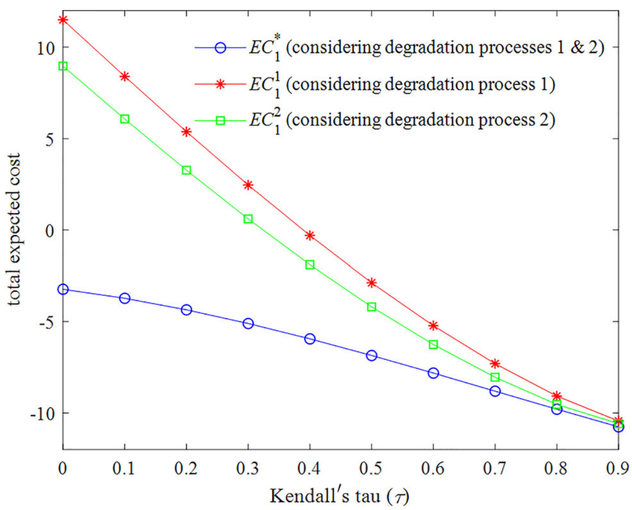

Figure 2. Three total expected costs under different levels of dependence.

dependence among degradation processes on optimal burn-in decisions. We also compare the total expected costs of the two burn-in models under different levels of dependence and different values of the inspection cost. In the sensitivity analysis, we use the same two dependent degradation processes used in the case study in Section 5, which are obtained from splitting the LED lamp dataset into two datasets. The Gumbel copula is used to model the dependence between the two degradation processes. The relationship between the copula parameter (λ) and Kendall's tau (τ) for the Gumbel copula is $\tau = 1 - 1/\lambda$. We use the same value of the warranty period and the same values of the cost parameters except for the inspection cost as presented in Section 5.2. Different levels of dependence between the two degradation processes and different values of the inspection cost are considered to investigate their impacts on optimal burn-in decisions.

6.1. Necessities of considering multiple dependent degradation processes in burn-in

We first examine whether it is worth considering multiple dependent degradation processes in burn-in. Ten different levels of dependence are considered, i.e., $\tau = 0, 0.1, \ldots, 0.9$. We compare the total expected costs of the burn-in models with and without consideration of multiple dependent degradation processes under different levels of dependence (τ). For each value of τ, we first obtain the optimal total expected cost of $\boldsymbol{M}_1$ (EC_1^*), which considers the two degradation processes during burn-in. We then find the optimal burn-in decision for the burn-in model considering only one degradation process. The costs resulted from the two burn-in decisions for degradation processes 1 and 2 are represented by EC_1^1 and EC_1^2, respectively. Figure 2 illustrates the three total expected costs under different levels of dependence. From Figure 2, we observe that the costs of the burn-in model with consideration of the two degradation processes are significantly lower than the costs of the burn-in model considering only one degradation process in all the scenarios. This result clearly shows that it is necessary to consider multiple dependent degradation processes in the burn-in planning for reduced costs. We also observe that the difference between EC_1^1 and EC_1^* and the difference between EC_1^2 and EC_1^* decrease as the level of dependence increases. This is because the joint survival probability converges to the marginal survival probability of one of the two degradation processes as τ approaches a value of one, leading to a smaller difference between the burn-in decisions with and without considering multiple degradation processes.

6.2. Impacts of the dependence level on optimal burn-in decisions

We now investigate the impacts of the dependence level on optimal burn-in decisions. Before analyzing such impacts, we first examine how the copula function changes as the level of dependence increases. This will help to understand the patterns of the optimal burn-in decisions under different levels of dependence. The relationship between Kendall's tau and copula function for the two-dimensional Gumbel copula is presented in Theorem 1.

Theorem 1. *Consider two bivariate Gumbel copula functions C_1 and C_2. C_1 has the association parameter λ_1 ($\lambda_1 \geq 1$) and Kendall's tau τ_1. C_2 has the association parameter λ_2 ($\lambda_2 \geq 1$) and Kendall's tau τ_2. If $\lambda_1 \leq \lambda_2$ (i.e., $\tau_1 \leq \tau_2$), we have $C_1(u, v) \leq C_2(u, v), \forall\ 0 \leq u, v \leq 1$.*

The proof of Theorem 1 makes use of two types of dependence orderings: the Positive Quadrant Dependence (PQD) ordering (Tchen 1980) and the Kendall stochastic ordering (Capéraa *et al.*, 1997). See detailed proof in Appendix B. Theorem 1 proves the nondecreasing pattern of a bivariate Gumbel copula function in Kendall's tau. It implies that the joint survival probability increases as the level of dependence increases. The same nondecreasing pattern can be found for the other four copulas mentioned in Section 5.1 numerically.

Table 7 presents the optimal burn-in decisions for the single-screening-point model ($\boldsymbol{M}_1$) under different levels of dependence. It can be seen that the optimal burn-in time t_b^* and the optimal burn-in thresholds γ^* increase as the level of dependence increases. This is because the survival probability of burn-in, i.e., $C(F_1(\gamma_1; x_1^0, t_b), F_2(\gamma_2; x_2^0, t_b))$, is nondecreasing in the level of dependence by Theorem 1. It indicates that burn-in for devices with a higher dependence level among degradation processes may require more time

Table 7. Optimal burn-in decisions of M_1 under different levels of dependence.

τ	t_b^*	γ^*	EC_1^*
0	8.13	(7.56, 11.38)	−3.23
0.1	9.76	(8.50, 12.63)	−3.72
0.2	11.07	(9.25, 13.50)	−4.36
0.3	12.02	(9.75, 14.25)	−5.11
0.4	12.42	(10.03, 14.63)	−5.95
0.5	12.88	(10.31, 15.03)	−6.86
0.6	13.00	(10.44, 15.25)	−7.82
0.7	13.53	(10.72, 15.63)	−8.81
0.8	13.77	(10.88, 15.88)	−9.80
0.9	14.28	(50.00, 16.06)	−10.76

Table 8. Optimal burn-in decisions of M_2 under different levels of dependence.

τ	q	μ^*	γ^{1*}	γ^{2*}	γ^{3*}	EC_2^*
0	3	5.41	(7.06, 12.25)	(9.81, 14.88)	(10.81, 16.25)	−3.81
0.1	3	5.70	(7.38, 11.88)	(10.19, 14.50)	(11.25, 16.75)	−4.49
0.2	3	6.32	(7.88, 13.75)	(11.88, 15.25)	(11.97, 17.63)	−5.23
0.3	3	7.30	(9.63, 13.63)	(11.69, 17.38)	(13.94, 17.75)	−6.14
0.4	3	7.88	(9.06, 15.25)	(12.25, 18.94)	(14.50, 19.50)	−7.15
0.5	3	6.71	(8.50, 13.75)	(12.50, 16.25)	(12.66, 19.63)	−8.11
0.6	3	8.43	(10.5, 17.03)	(13.75, 18.75)	(14.09, 20.19)	−9.04
0.7	3	7.60	(12.19, 15.69)	(12.31, 18.25)	(13.56, 19.63)	−10.23
0.8	2	13.30	(13.75, 17.63)	(14.56, 21.75)	–	−11.86
0.9	2	13.55	(13.88, 17.91)	(14.75, 19.97)	–	−12.03

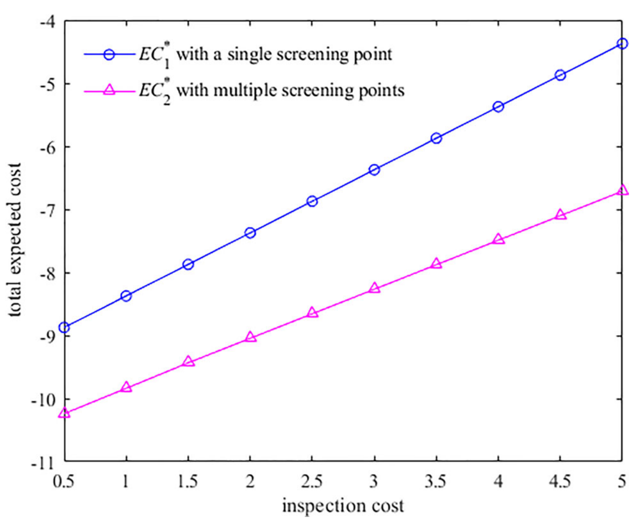

Figure 3. Optimal total costs under different values of the inspection cost.

to identify weak units, and longer burn-in time consequently leads to higher burn-in thresholds.

The optimal burn-in decisions under different levels of dependence for the multi-screening-point model (M_2) are summarized in Table 8. From Table 8, we observe a similar pattern that the optimal time interval between two consecutive screening points increases in most cases as the dependence level increases. We also observe that the optimal number of screening points reduces from three to two when the dependence level becomes higher. Moreover, comparing the costs in Table 7 with those in Table 8, we can see that the multi-screening-point model outperforms the single-screening-point model in terms of the total expected cost under all levels of dependence considered. Therefore, burn-in with multiple screening points can be more cost beneficial.

6.3. Impacts of the inspection cost on optimal total expected costs

We further compare the optimal total expected costs of the single-screening-point model (M_1) with those of the multi-screening-point model (M_2) under different values of the inspection cost. Ten different values of the inspection cost are considered, i.e., $c_0 = 0.5, 1, \ldots, 5$. Figure 3 shows the optimal total expected costs of M_1 and M_2 (i.e., EC_1^* and EC_2^*) in the 10 scenarios considered. It can be seen that the total expected costs of burn-in with multiple screening points are lower than the costs of burn-in with a single screening point under all values of the inspection cost considered. In addition, the cost difference between the two models becomes larger as the inspection cost increases. This is because burn-in with multiple screening points can potentially save more burn-in cost by eliminating weak units at earlier screening points when the inspection cost is higher.

7. Conclusion

In this article, we consider the problem of designing optimal burn-in policies for devices subject to multiple dependent degradation processes with unit-to-unit heterogeneity. We use the copula method to analyze the dependent structure among multiple degradation processes and model the unit-level heterogeneity as random effects. A two-stage estimation method is developed to estimate univariate parameters for each marginal degradation process and copula parameter(s) effectively. To reduce the heterogeneity, we propose two degradation-based burn-in models, one with a single screening point and the other with multiple equi-spaced screening points. Efficient algorithms are designed to find optimal burn-in decisions. Experimental data from LED lamps is used to demonstrate a bivariate degradation model. Impacts of parameter uncertainties on optimal burn-in decisions are investigated. We further conduct sensitivity analyses using the two dependent degradation processes in the LED lamp example. Our results show that it is necessary to consider multiple dependent degradation processes in burn-in. Additionally, a higher level of dependence between the two degradation processes often results in longer burn-in time and higher burn-in thresholds for the two burn-in models. For the multiple-screening-point model, a higher level of dependence can also lead to fewer screening points. The results also show that substantial cost savings can be achieved by performing multiple screening points during burn-in.

In this article, we treat the accelerated LED lamp data as it were in-field use data during the warranty period. The future work will consider optimal burn-in for multiple dependent degradation processes using data obtained from accelerated degradation tests and with extrapolation to a normal use condition. It is also worth considering sequential inspection instead of periodic inspection as considered in this article for the burn-in model with multiple screening points. In addition, to explore whether the dependence among different failure processes varies in time, it is interesting to extend constant copulas to time-varying copulas.

Funding

This work was supported in part by the U.S. National Science Foundation under Award 1855408.

Notes on contributors

Yue Shi is a PhD student in Department of Industrial, Manufacturing & Systems Engineering at Texas Tech University. She received her BS degree in Ecommerce from Guangdong University of Foreign Studies, China and MS degree in management science and engineering from Sun Yat-sen University, China. Her research interests include decision-making under uncertainty, maintenance optimization, and multivariate degradation modeling. She is a student member of INFORMS.

Dr. Yisha Xiang is an assistant professor in the Department of Industrial, Manufacturing & Systems Engineering at Texas Tech University. Her current research and teaching interests involves reliability modeling and optimization, maintenance optimization, and decision-making under uncertainty. Her research has been funded by the National Science Foundation (NSF), including a CAREER grant, and industry. She has published articles in refereed journals, such as *INFORMS Journal on Computing, IISE Transactions, European Journal of Operational Research,* and *IEEE Transactions on Reliability*. She was the recipient of the Ralph A. Evans/P.K. McElroy Award for the best paper at the 2013 Reliability and Maintainability Symposium, and Stan Oftshun Best Paper Award from Society of Reliability Engineers in 2013 and 2017. She received her BS in industrial engineering from Nanjing University of Aero. & Astro., China, and MS and PhD in industrial engineering from University of Arkansas. She is an associate editor for *IEEE Transactions Automation Science and Engineering*, and she is a member of IISE and INFORMS.

Ying Liao is a PhD student in Department of Industrial, Manufacturing & Systems Engineering at Texas Tech University. She received her BS and MS in statistics from Sun Yat-sen University, China. Her research interest includes reliability modeling, statistical machine learning, and Bayesian analysis. She is a student member of INFORMS.

Zhicheng Zhu is a PhD candidate in Department of Industrial, Manufacturing & Systems Engineering at Texas Tech University. He received his BS and MS in electrical engineering from Sun Yat-sen University, China. His main research interests are maintenance optimization, decision-making under uncertainty, and reliability modeling. He is a student member of INFORMS.

Yili Hong received his PhD in statistics from Iowa State University in 2009. He is professor of statistics at Virginia Tech. His research interests include machine learning and engineering applications, reliability analysis, and spatial statistics. He has more than 90 publications in publications such as *Journal of the American Statistical Association, Annals of Applied Statistics, Technometrics,* and *IEEE Transactions on Reliability*. He is currently an associate editor for *Technometrics* and *Journal of Quality Technology*. He is an elected member of International Statistical Institute. He won the 2011 DuPont Young Professor Award, and the 2016 Frank Wilcoxon Prize in statistics.

References

Andersen, E.W. (2005) Two-stage estimation in copula models used in family studies. *Lifetime Data Analysis*, **11**(3), 333–350.

Capéraa, P., Fougeres, A.-L. and Genest, C. (1997) A stochastic ordering based on a decomposition of Kendall's Tau, in *Distributions with Given Marginals and Moment Problems*, Springer, Dordrecht, pp. 81–86.

Cha, J.H. and Pulcini, G. (2016) Optimal burn-in procedure for mixed populations based on the device degradation process history. *European Journal of Operational Research*, **251**(3), 988–998.

Chaluvadi, V. (2008) Accelerated life testing of electronic revenue meters. PhD thesis, Clemson University, Clemson, SC, USA.

Cools, R. (2002) Advances in multidimensional integration. *Journal of Computational and Applied Mathematics*, **149**(1), 1–12.

Elwany, A.H., Gebraeel, N.Z. and Maillart, L.M. (2011) Structured replacement policies for components with complex degradation processes and dedicated sensors. *Operations Research*, **59**(3), 684–695.

Embrechts, P., Lindskog, F. and McNeil, A. (2001) Modelling dependence with copulas. Rapport technique, Département de mathématiques, Institut Fédéral de Technologie de Zurich, Zurich.

Fang, G., Pan, R. and Hong, Y. (2018) A copula-based multivariate degradation analysis for reliability prediction, in *Proceedings of the 2018 Annual Reliability and Maintainability Symposium,* IEEE, Reno, NV, USA, pp. 1–7.

Fang, G., Pan, R. and Hong, Y. (2020) Copula-based reliability analysis of degrading systems with dependent failures. *Reliability Engineering & System Safety*, **193**, 1–19.

Genest, C. and MacKay, R.J. (1986) Copules Archimédiennes et familles de lois bidimensionnelles dont les marges sont données. *Canadian Journal of Statistics*, **14**(2), 145–159.

Genest, C. and Rivest, L.-P. (1993) Statistical inference procedures for bivariate Archimedean copulas. *Journal of the American Statistical Association*, **88**(423), 1034–1043.

Hao, H., Su, C. and Li, C. (2015) LED lighting system reliability modeling and inference via random effects gamma process and copula function. *International Journal of Photoenergy*, 1–8.

Joe, H. (2005) Asymptotic efficiency of the two-stage estimation method for copula-based models. *Journal of Multivariate Analysis*, **94**(2), 401–419.

Joe, H. and Xu, J.J. (1996) The estimation method of inference functions for margins for multivariate models, Tech. Rep. No. 166, Department of Statistics, University of British Columbia, Canada.

Lawless, J. and Crowder, M. (2004) Covariates and random effects in a gamma process model with application to degradation and failure. *Lifetime Data Analysis*, **10**(3), 213–227.

Li, C. and Hao, H. (2016) A copula-based degradation modeling and reliability assessment. *Engineering Letters*, **24**(3), 295–300.

Nelsen, R.B. (2007) *An Introduction to Copulas*, Springer, New York.

Pan, Z. and Balakrishnan, N. (2011) Reliability modeling of degradation of products with multiple performance characteristics based on gamma processes. *Reliability Engineering & System Safety*, **96**(8), 949–957.

Pan, Z., Balakrishnan, N. and Sun, Q. (2011) Bivariate constant-stress accelerated degradation model and inference. *Communications in Statistics–Simulation and Computation*, **40**(2), 247–257.

Pan, Z., Balakrishnan, N., Sun, Q. and Zhou, J. (2013) Bivariate degradation analysis of products based on Wiener processes and copulas. *Journal of Statistical Computation and Simulation*, **83**(7), 1316–1329.

Pan, Z. and Sun, Q. (2014) Optimal design for step-stress accelerated degradation test with multiple performance characteristics based on gamma processes. *Communications in Statistics-Simulation and Computation*, **43**(2), 298–314.

Peng, W., Li, Y.-F., Yang, Y.-J., Zhu, S.-P. and Huang, H.-Z. (2016) Bivariate analysis of incomplete degradation observations based on inverse Gaussian processes and copulas. *IEEE Transactions on Reliability*, **65**(2), 624–639.

Sakamoto, Y., Ishiguro, M. and Kitagawa, G. (1986) *Akaike Information Criterion Statistics*, Reidel, Dordrecht, The Netherlands, p. 1.

Sari, J., Newby, M., Brombacher, A. and Tang, L.C. (2009) Bivariate constant stress degradation model: LED lighting system reliability estimation with two-stage modelling. *Quality and Reliability Engineering International*, **25**(8), 1067–1084.

Tchen, A.H. (1980) Inequalities for distributions with given marginals. *The Annals of Probability*, **8**(4), 814–827.

Tsai, C.-C., Tseng, S.-T. and Balakrishnan, N. (2011) Optimal burn-in policy for highly reliable products using gamma degradation process. *IEEE Transactions on Reliability*, **60**(1), 234–245.

Tseng, S.-T. and Peng, C.-Y. (2004) Optimal burn-in policy by using an integrated Wiener process. *IIE Transactions*, **36**(12), 1161–1170.

Tseng, S.T. and Tang, J. (2001) Optimal burn-in time for highly reliable products. *International Journal of Industrial Engineering-Theory Applications and Practice*, **8**(4), 329–338.

Tseng, S.-T., Tang, J. and Ku, I.-H. (2003) Determination of burn-in parameters and residual life for highly reliable products. *Naval Research Logistics*, **50**(1), 1–14.

Wang, X. (2010) Wiener processes with random effects for degradation data. *Journal of Multivariate Analysis*, **101**(2), 340–351.

Wang, X. and Xu, D. (2010) An inverse Gaussian process model for degradation data. *Technometrics*, **52**(2), 188–197.

Wang, Y. and Pham, H. (2012) Modeling the dependent competing risks with multiple degradation processes and random shock using time-varying copulas. *IEEE Transactions on Reliability*, **61**(1), 13–22.

Yang, Q., Hong, Y., Zhang, N. and Li, J. (2017) A copula-based trend-renewal process model for analysis of repairable systems with multitype failures. *IEEE Transactions on Reliability*, **66**(3), 590–602.

Ye, Z.-S., Xie, M., Tang, L.-C. and Chen, N. (2014) Semiparametric estimation of gamma processes for deteriorating products. *Technometrics*, **56**(4), 504–513.

Ye, Z.-S., Xie, M., Tang, L.-C. and Shen, Y. (2012) Degradation-based burn-in planning under competing risks. *Technometrics*, **54**(2), 159–168.

Zhang, M., Ye, Z. and Xie, M. (2015) Optimal burn-in policy for highly reliable products using inverse Gaussian degradation process, in *Engineering Asset Management-Systems, Professional Practices and Certification*, Springer, pp. 1003–1011.

Zhou, J., Pan, Z. and Sun, Q. (2010) Bivariate degradation modeling based on gamma process, in *Proceedings of the World Congress on Engineering* (Vol. **3**), International Association of Engineers (IAENG), London, UK, pp. 1783–1788.

Appendices

A. Proof of Proposition 2

Proof. The total expected cost $EC_1(t_b, \gamma)$ of the burn-in model with consideration of a single degradation process is given by

$$\begin{aligned} EC_1(t_b,\gamma) =& c_0 + c_b t + c_d + (c_f - c_d)F(\gamma; x^0, 0, t_b) \\ & - (c_f + r_w)\int_0^{\gamma} F(\xi; u, t_b, t_b + t_w) f(u; x^0, 0, t_b)\, du. \end{aligned} \tag{20}$$

Taking the derivative of Equation (20) in terms of γ and setting it to zero, we obtain

$$\frac{\partial}{\partial\gamma} EC_1|_{\gamma=\gamma^*} = f(\gamma; x^0, 0, t_b)[(c_f - c_d) - (c_f + r_w)F(\xi; \gamma, t_b, t_b + t_w)] = 0.$$

Since the first term on the right-hand side is always positive, we determine the sign of the second-order derivative as

$$\frac{\partial^2}{\partial\gamma^2} EC_1|_{\gamma=\gamma^*} = (c_f + r_w) f(\gamma; x^0, 0, t_b) f(\xi; \gamma, t_b, t_b + t_w) > 0.$$

Therefore, the minimum of EC_1 is achieved when $\partial EC_1/\partial\gamma$ equals zero. Because it is assumed that $c_d \le c_f$ and $-c_d \le r_w$, we have $0 \le \rho \le 1$, where $\rho = (c_f - c_d)/(c_f + r_w)$. Therefore, the optimal burn-in threshold is determined by $\rho = F(\xi; \gamma^*, t_b, t_b + t_w)$. □

B. Proof of Theorem 1

Proof. To prove Theorem 1, we first introduce the definitions of two types of dependence orderings: the PQD ordering (Tchen, 1980) and the Kendall stochastic ordering (Capéraa *et al.*, 1997), which are given as follows:

$$C_1 \prec_{PQD} C_2 \iff C_1(u,v) \le C_2(u,v), \ \forall u, v \in [0,1], \tag{21}$$

$$C_1 \prec_K C_2 \iff K_2(t) \le K_1(t), \forall t \in [0,1], \tag{22}$$

where $\prec_{PQD}$ and $\prec_K$ represent the PQD ordering and the Kendall stochastic ordering, respectively. Note that $K_i(t)$ denotes the Kendall distribution function of C_i, i.e., $K_i(t) = \Pr\{C_i(u,v) \le t\}$, $t \in [0,1]$, $i = 1$, 2. Moreover, the Kendall distribution function of the Archimedean copula with a generator function $\phi : (0,1] \to [0,\infty)$ is given by (Genest and Rivest, 1993)

$$K_\phi(t) = t - \frac{\phi(t)}{\phi'(t)}, 0 < t \le 1. \tag{23}$$

Given two bivariate Archimedean copulas C_1 and C_2, it has been proved by Genest and MacKay (1986) that Equation (22) is the sufficient condition of Equation (21). The implication is given as follows:

$$C_1 \prec_K C_2 \Rightarrow C_1 \prec_{PQD} C_2. \tag{24}$$

Based on the previous analysis of the two dependence orderings, we then begin the proof of Theorem 1. The Kendall's tau of Gumbel copula is $\tau = 1 - 1/\lambda$, which increases as λ increases. The generator function of the Gumbel copula is $\phi(t) = (-\log t)^\lambda$, where $0 < t \le 1$. We then show that the Kendall distribution function of the Gumbel copula is strictly decreasing in λ. The corresponding Kendall distribution function is given as follows:

$$K_\lambda(t) = t - \frac{t \log t}{\lambda}, \tag{25}$$

which is decreasing in λ. Thus, by Equations (21), (22), and (24), the proof is summarized as follows

$$\begin{aligned} & \lambda_1 \le \lambda_2 \Rightarrow \tau_1 \le \tau_2 \Rightarrow K_{\lambda_2} \le K_{\lambda_1} \\ & \iff C_1 \prec_K C_2 \Rightarrow C_1 \prec_{PQD} C_2 \iff C_1 \le C_2. \end{aligned} \tag{26}$$

□